Performance-Guaranteed Solutions for Multi-Agent Optimal Coverage Problems using Submodularity, Curvature, and Greedy Algorithms

Shirantha Welikala and Christos G. Cassandras

***Abstract*— We consider a class of multi-agent optimal coverage problems in which the goal is to determine the optimal placement of a group of agents in a given mission space so that they maximize a coverage objective that represents a blend of individual and collaborative event detection capabilities. This class of problems is extremely challenging due to the non-convex nature of the mission space and of the coverage objective. With this motivation, we propose to use a *greedy algorithm* as a means of getting feasible coverage solutions efficiently. Even though such greedy solutions are suboptimal, the *submodularity* (diminishing returns) property of the coverage objective can be exploited to provide performance bound guarantees. Moreover, we show that improved performance bound guarantees (beyond the standard (1-1/e) performance bound) can be established using various *curvature measures* of the coverage problem. In particular, we provide a brief review of all existing popular applicable curvature measures, including a recent curvature measure that we proposed, and discuss their effectiveness and computational complexity, in the context of optimal coverage problems. We also propose novel computationally efficient techniques to estimate some curvature measures. Finally, we provide several numerical results to support our findings and propose several potential future research directions.**

I. Introduction

Our research focuses on multi-agent optimal coverage problems, which often arise in critical applications such as (but not limited to) surveillance, security, agriculture, and search and rescue [2], [8]. In these problems, the overall goal is to find an effective placement (decision variable) for the agent team so that they can optimally "cover" (i.e., individually and/or collaboratively detect events of interest randomly occurring in) the mission space.

Due to their wide applicability, several variants of multi-agent optimal coverage problems have been extensively studied in the literature [6], [12], [15], [16]. Typically, these are formulated as continuous optimization problems inspired by real-world conditions. However, their corresponding solutions are computationally expensive unless significant simplifying assumptions are made regarding the particular coverage problem setup. This is mainly due to the overall challenging nature of coverage problems resulting from the often non-linear, non-convex, and non-smooth coverage objectives and non-convex mission spaces involved.

In this paper, we adopt an alternative approach that has been taken in the literature [9], [10], and formulate the multi-agent optimal coverage problem as a combinatorial optimization problem by discretizing the associated mission/decision space. The coverage objective function, in this setting, is proven to be a *submodular* set function. In other words, the coverage objective function shows *diminishing returns* when the deployed set of agents is expanded. While this combinatorial formulation simplifies the coverage problem to a certain level, it now takes the form of a submodular maximization problem that is known to be NP-hard [4], [7].

Greedy algorithms are commonly used to solve submodular maximization problems due to their simplicity and computational efficiency. Most importantly, the resulting greedy solutions, even though suboptimal, entertain performance bounds that characterize their proximity to the global optimal solution. The seminal work in [7] has established a $1-(1-\frac{1}{N})^N$ performance bound, which becomes $(1-\frac{1}{e}) \simeq 0.6321$ as the solution set size (i.e., in the coverage problem, the number of agents) $N \to \infty$. Hence the greedy solution is not worse than 63.21% of the global optimal solution. Recent literature has focused on developing improved performance bounds beyond this fundamental performance bound.

To this end, various *curvature measures* have been proposed to further characterize any given submodular maximization problem [3], [5], [11], [14]. These curvature measures provide corresponding performance bounds, which may or may not significantly improve upon the fundamental performance bound - depending on the nature of the considered problem/application. However, often these curvature measures are computationally expensive to evaluate. Moreover, given the variety of curvature measures available and the variations in their effectiveness with respect to problem parameters, selecting a curvature measure that is likely to provide significantly improved performance bounds for a particular application is challenging.

Our previous work in [10] considered a widely studied multi-agent optimal coverage problem (e.g., see [12], [16]) and showed that the *total curvature* [3] and *elemental curvature* [11] can collectively provide improved performance bounds. The subsequent work in [9] considered a slightly different coverage problem with a team selection element and showcased the effectiveness of the *greedy curvature* [3] and *partial curvature* [5] in providing improved performance bounds. Our most recent work in [14] considered the general submodular maximization problem and proposed a new curvature measure called the *extended greedy curvature*. Then, using the coverage problem, its effectiveness compared to all other curvature measures mentioned above was illustrated. In this paper, we consider a more general coverage problem than before and investigate the effectiveness and complexity of all these curvature measures through theoretical analysis, development, and numerical experiments.

In particular, our contributions are as follows: **(1)** We consider a more general coverage problem (compared to those in [10], [14]); **(2)** Submodularity and several other key properties of the considered coverage problem are established; **(3)** We review five curvature measures that are applicable to the considered coverage problem (to the best of our knowledge, this review is exhaustive); **(4)** Special properties and techniques for numerical evaluation of some complex curvature measures for coverage problems are discussed; **(5)** We detail the effectiveness complexity of different curvature metrics with respect to various coverage problem parameters; and **(6)** We implement the proposed coverage problem setup in a simulation environment and evaluate different curvature measures and their performance bounds under different problem conditions.

Organization: We introduce the considered coverage problem in Section II. Some notations, preliminary concepts, and the proposed greedy solution are reported in Section III. Different curvature measures found in the literature, along with discussions on their effectiveness and complexity in the context of optimal coverage problems, are provided in Section IV. A summary and some future research directions are given in Section V. Several numerical results are reported in Section VI before concluding the paper in Section VII.

II. Multi-Agent Optimal Coverage Problem

We begin by providing the details of the considered multi-agent optimal coverage problem. The goal of the considered coverage problem is to determine an optimal placement for a given team of agents (e.g., sensors, cameras, guards, etc.) in a given mission space that maximizes the probability of detecting events that occur randomly over the mission space.

We model the *mission space* Ω as a convex polytope in $\mathbb{R}^n$ that may also contain h polytopic (and possibly non-convex) *obstacles* $\{\Psi_i : \Psi_i \subset \Omega, i \in \mathbb{N}_h\}$ (note that: $\mathbb{N}_n \triangleq \{1,2,\ldots,n\}$). The obstacles: (1) limit the agent placement to the feasible space $\Phi \triangleq \Omega \backslash \cup_{i\in\mathbb{N}_h} \Psi_i$, (2) constrain the sensing capabilities of agents via obstructing their line of sight, and (3) are in areas where no events of interest occur.

To model the likelihood of random *events* occurring over the mission space, an *event density function* $R : \Omega \to \mathbb{R}_{\geq 0}$ is used, where $R(x) = 0, \forall x \notin \Phi$ and $\int_\Omega R(x)dx < \infty$. If no prior information on $R(x)$ is known, one can use $R(x) = 1, \forall x \in \Phi$.

To detect these random events, N *agents* are to be placed inside the feasible space Φ, where their placement (i.e., the decision variable) is denoted by a matrix $s \triangleq [s_1, s_2, \ldots, s_N] \in \mathbb{R}^{m\times N}$ or a set $S \triangleq \{s_i : i \in \mathbb{N}_N, s_i \in \mathbb{R}^m\}$, where each $s_i, i \in \mathbb{N}_N$ represents an agent placement such that $s_i \in \Phi$.

The ability of an agent to *detect* events is limited by its sensing capabilities and visibility obstruction from obstacles. In particular, for an agent at $s_i \in \Phi$, its *visibility region* is defined as $V(s_i) \triangleq \{x : (qx + (1-q)s_i) \in \Phi, \forall q \in [0,1]\}$. Moreover, agents are assumed to be homogeneous in their *sensing capabilities*. In particular, each agent has a finite *sensing radius* $\delta \in \mathbb{R}_{\geq 0}$ and *sensing decay rate* $\lambda \in \mathbb{R}_{\geq 0}$ that defines the probability of an agent at $s_i \in \Phi$ detecting an event at $x \in \Phi$ via a *sensing function* of the form

$$p(x, s_i) \triangleq e^{-\lambda \|x-s_i\|} \cdot \mathbf{1}_{\{x\in V(s_i)\}}. \tag{1}$$

Given agent team placement s (or, equivalently, S), their ability to detect an event at $x \in \Phi$ is described by a *detection function* $P(x,s)$. For this, the *joint detection function*:

$$P_J(x,s) \triangleq 1 - \prod_{i\in\mathbb{N}_N} (1 - p(x, s_i)), \tag{2}$$

is a popular choice that represents the probability of detection by at least one agent (assuming independently detecting agents). Moreover, the *max detection function* given by

$$P_M(x,s) \triangleq \max_{i\in\mathbb{N}_N} p(x, s_i), \tag{3}$$

is also a widely used choice that represents the maximum probability of detection by any agent. The following remark summarizes the pros and cons of using (2) or (3) as $P(x,s)$.

Remark 1: The joint detection function (2) offers a complete but computationally intensive view of coverage by combining all agent efforts. Thus it is suited for scenarios where collaborative detection is needed. Conversely, the max detection function (3) focuses on the top-performing agent at each point, providing a simpler yet non-smooth and potentially under-utilizing approach. Thus it is suited for scenarios where individual yet maximum detection is needed. Choosing between these depends on the application's needs, agent characteristics, and available computational resources.

Motivated by the contrasting nature of the joint and max detection functions, we propose the detection function

$$P(x,s) \triangleq \theta P_J(x,s) + (1-\theta) P_M(x,s), \tag{4}$$

where $\theta \in [0,1]$ is a predefined weight (e.g., see Fig. 1).

Using the defined event density and detection functions, the considered optimal coverage problem can be stated as

$$s^* = \underset{s:s_i\in\Phi, i\in\mathbb{N}_N}{\arg\max}\ H(s) \triangleq \int_\Omega R(x)P(x,s)dx, \tag{5}$$

where $H(s)$ (or equivalently, $H(S)$) is the *coverage function*.

Continuous Optimization Approach: The optimal coverage problem (5) involves a non-convex feasible space and a non-convex, non-linear, and non-smooth objective function. Therefore, it is extremely difficult to solve without using: (1) standard global optimization solvers that are computationally expensive, or (2) systematic gradient-based solvers that require extensive domain knowledge.

Combinatorial Optimization Approach: Motivated by the said challenges, here we take a combinatorial optimization approach to solve (5). This requires reformulating (5) as a set function maximization problem (in set variable S).

First, we discretize the feasible space Φ formulating a *ground set* $X = \{x_l : x_l \in \Phi, l \in \mathbb{N}_M\}$. Second, we replace the matrix variable s with the *set variable* $S \triangleq \{s_i : i \in \mathbb{N}\}$ in detection and coverage functions defined in (2)-(5), to obtain their respective set detection and set coverage functions. To limit the cardinality of S (denoted by $|S|$) to N, we introduce the constraint $S \in \mathscr{I}^N \triangleq \{Y : Y \subseteq X, |Y| \leq N\}$. Finally, we restate the optimal coverage problem (5) as a set function maximization problem:

$$S^* = \underset{S\in\mathscr{I}^N}{\arg\max}\ H(S) \triangleq \int_\Omega R(x)P(x,S)dx. \tag{6}$$

Remark 2: A set system form $(X,\mathscr{I}^N)$ is known as a *uniform matroid* of rank N, and a set constraint $S\in\mathscr{I}^N$ is known as a uniform matroid constraint of rank N [14].

Clearly, the size of the search space of (6) is combinatorial as $|\mathscr{I}^N|=\sum_{r=0}^{N}\binom{M}{r}$. Therefore, obtaining an optimal solution S^* for it is impossible without significant simplifying assumptions. Hence our goal here is to obtain a candidate solution for (6) (say S^G) in an efficient manner with some guarantees on its coverage performance $H(S^G)$ with respect to the optimal coverage performance $H(S^*)$.

To efficiently obtain such a candidate solution, we use a vanilla *greedy algorithm* as given in Alg. 1. Note that it uses the notion of *marginal coverage function* defined as

$$\Delta H(y|S^{i-1})\triangleq H(S^{i-1}\cup\{y\})-H(S^{i-1}), \tag{7}$$

to iteratively determine optimal individual agent placements until N such agent placements have been chosen.

Motivated by the linear relationship between the set coverage function $H(S)$ (6) and set detection function $P(x,S)$ (4), we define the notion of *marginal detection function* as

$$\Delta P(x,y|S^{i-1})\triangleq P(x,S^{i-1}\cup\{y\})-P(x,S^{i-1}). \tag{8}$$

Through (6), it is easy to see that a similar linear relationship also exists between the marginal functions $\Delta H(y|S)$ (7) and $\Delta P(x,y|S)$ (8). In the sequel, we exploit these linear relationships to conclude certain set function properties of $H(S)$ using those of $P(x,S)$ and $\Delta P(x,y|S)$.

Finally, we point out that, in the sequel, the notations in (7) and (8) will be used more liberally by replacing y and S^{i-1} respectively with sets A and B, where $A,B\subseteq X$ (e.g., see Th. 2). Also, the notation $S^i\triangleq\{s^1,s^2,\ldots,s^i\}$ used to represent the greedy solution obtained after i greedy iterations in Alg. 1 will be used more liberally for any $i\in\mathbb{N}_M^0$ (e.g., see (30)).

Algorithm 1 The greedy algorithm to solve (6)

```
1: i = 0; S^i = ∅;          ▷ Greedy iteration index and solution
2: for i = 1,2,3,...,N do
3:     s^i = argmax_{y: S^{i-1} ∪ {y} ∈ I^N} ΔH(y|S^{i-1});  ▷ New item
4:     S^i = S^{i-1} ∪ {s^i};              ▷ Append the new item
5: end for
6: S^G := S^N; Return S^G;
```

III. The Greedy Solution with Performance Bound Guarantees

In this section, we show that the greedy solution S^G given by Alg. 1 for the optimal coverage problem (6) not only efficient but also entertains performance guarantees with respect to the global optimal performance $H(S^*)$. For this, we first need to introduce some standard set function properties.

Definition 1: [14] Let $F:2^Y\to\mathbb{R}$ be an arbitrary set function defined over a finite ground set Y, and $\Delta F(y|A)\triangleq F(A\cup\{y\})-F(A)$ be the corresponding marginal gain function. This set function F is: **(1)** *normalized* if $F(\emptyset)=0$; **(2)** *monotone* if $\Delta F(y|A)\geq 0$ for all y,A where $A\subset Y$ and $y\in Y\backslash A$, or equivalently, if $F(B)\leq F(A)$ for all B,A where $B\subseteq A\subseteq Y$; **(3)** *submodular* if $\Delta f(y|A)\leq\Delta f(y|B)$ for all y,A,B where $B\subseteq A\subset Y$ and $y\in Y\backslash A$, or equivalently, if $F(A\cup B)+F(A\cap B)\leq F(A)+F(B)$ for all $A,B\subseteq Y$; **(4)** a *polymatroid* set function if all the above properties hold [1].

The following lemma and the theorem establish that the coverage function $H(S)$ in (6) is a polymatroid set function.

Lemma 1: With respect to a common ground set, any positive linear combination of arbitrary polymatroid set functions is also a polymatroid set function.

Proof: The proof directly follows from: (1) considering $F_1,F_2,\ldots,F_n$ to be n polymatroid set functions defined over a common ground set, (2) defining $F\triangleq\sum_{i\in\mathbb{N}_n}\alpha_iF_i$, where $\alpha_i\geq 0,\forall i\in\mathbb{N}_n$, and (3) testing respective conditions in Def. 1. A more detailed proof can be found in [13]. ■

Theorem 1: The set coverage function $H(S)$ in (6) is a polymatroid set function.

Proof: Note that $H(S)$ is a linear combination of set detection function components $P_J(x,S)$ (2) and $P_M(x,S)$ (3) with respect to the common ground set X. Thus, under Lm. 1, we only have to prove $P_J(x,S)$ and $P_M(x,S)$ are polymatroid set functions with respect to any feasible space point $x\in\Phi$.

We start by considering $P_J(x,S)$. By definition, $P_J(x,\emptyset)=0$, and thus, it is normalized. The corresponding marginal function $\Delta P_J(x,y|A)=P_J(x,A\cup\{y\})-P_J(x,A)=-\prod_{s_i\in A\cup\{y\}}(1-p(x,s_i))+\prod_{s_i\in A}(1-p(x,s_i))$, leading to:

$$\Delta P_J(x,y|A)=p(x,y)\prod_{s_i\in A}(1-p(x,s_i)), \tag{9}$$

for any $A\subset X$ and $y\in X\backslash A$. Therefore, $\Delta P_J(x,y|A)\geq 0$, which implies that $P_J(x,S)$ is monotone. Note also that the product term in (9) diminishes with the growth of the set A. Therefore, $\Delta P_J(x,y|A)\leq\Delta P_J(x,y|B)$, for all y,A,B where $B\subseteq A\subset X$ and $y\in Y\backslash A$. Hence $P_J(x,S)$ is submodular, and thus, it is also a polymatroid set function.

Finally, we consider $P_M(x,S)$. Note that $P_M(x,\emptyset)=0$, which implies that it is normalized. The corresponding marginal function $\Delta P_M(x,y|A)=P_M(x,A\cup\{y\})-P_M(x,A)=\max_{s_i\in A\cup\{y\}}p(x,s_i)-\max_{s_i\in A}p(x,s_i)$, leading to:

$$\Delta P_M(x,y|A)=\max\{0,p(x,y)-\max_{s_i\in A}p(x,s_i)\}, \tag{10}$$

for any $A\subset X$ and $y\in X\backslash A$. Therefore, $\Delta P_M(x,y|A)\geq 0$, implying that $P_M(x,S)$ is monotone. Note also that the second inner term in (10) diminishes with the growth of the set A. Thus, $\Delta P_M(x,y|A)\leq\Delta P_M(x,y|B)$, for all y,A,B where $B\subseteq A\subset X$ and $y\in Y\backslash A$. Hence $P_M(x,S)$ is submodular, and thus, it is a polymatroid set function. This completes the proof. ■

This polymatroid nature of set coverage function $H(S)$ (6) enables establishing *performance bounds* (denoted by β) for the greedy solution S^G (given by Alg. 1). Formally, a performance bound is defined as a theoretically established lower bound for the ratio $\frac{H(S^G)}{H(S^*)}$, i.e., $\beta\leq\frac{H(S^G)}{H(S^*)}$. Having a performance bound $\beta\simeq 1$ implies that the performance of the greedy solution S^G is close to that of the global optimal solution S^*. Thus, β is an indicator of the effectiveness of the greedy approach to solving the coverage problem (6).

The seminal work [7] has established a performance bound (henceforth called the *fundamental performance bound*, and denoted by β_f) for polymatroid set function maximization problems. This, in light of Th. 1, is applicable to the optimal coverage problem (6) as:

$$\beta_f \triangleq 1 - \left(1 - \frac{1}{N}\right)^N \leq \frac{H(S^G)}{H(S^*)}. \tag{11}$$

While β_f decreases with the number of agents N, it is lower-bounded by $1 - \frac{1}{e} \simeq 0.6321$, because $\lim_{N\to\infty} \beta_f = (1 - \frac{1}{e})$. This implies that the coverage performance of the greedy solution will always be not worse than 63.21% of the maximum achievable coverage performance.

As we will see in the next section, further improved performance bounds beyond β_f can be achieved by exploiting certain characteristics called *curvature measures* of the interested set function maximization problem.

Before moving on, we provide a theorem that establishes the polymatroid nature of the marginal coverage function $\Delta H(B|A)$ with respect to both of its set arguments A and B.

Theorem 2: For a fixed set $A \subset X$, the marginal coverage function $G_A(B) \triangleq \Delta H(B|A)$ is a polymatroid set function over $B \subseteq X\backslash A$. Also, for a fixed set $B \subset X$, the affine negated marginal coverage function $G_B(A) \triangleq -\Delta H(B|A) + H(B)$ is a polymatroid set function over $A \subseteq X\backslash B$.

Proof: Due to space constraints, the proof is omitted here, but can be found in [13]. ■

The above result further emphasizes the deep polymatroid features of optimal coverage problems. Moreover, as we will see in the sequel, it enables achieving computationally efficient estimates for some (otherwise computationally intractable) curvature measures discussed in the next section.

IV. Improved Performance Bound Guarantees using Curvature Measures

In this section, we discuss several improved performance bounds (i.e., closer to 1 compared to β_f in (11)) applicable for the greedy solution S^G given by Alg. 1 for the optimal coverage problem in (6). This is important as such an improved performance bound will accurately characterize the proximity of S^G to S^* and thus enable making informed decisions regarding spending extra resources (e.g., computational power, agents, and sensing capabilities) to seek further improved coverage solutions beyond S^G.

In particular, curvature measures are used to obtain such improved performance bounds, and they are dependent purely on the underlying objective function, the ground set, and the feasible space, which, in the considered optimal coverage problem, are $H(S)$, X, and $\mathscr{I}^N$, respectively. Here, we will review five established curvature measures and their respective performance bounds, outlining their characteristics, strengths, and weaknesses in the context of optimal coverage problems (6).

A. Total Curvature [3]

By definition, the *total curvature* of (6) is given by

$$\alpha_t \triangleq \max_{y\in X}\left[1 - \frac{\Delta H(y|X\backslash\{y\})}{\Delta H(y|\emptyset)}\right]. \tag{12}$$

The corresponding performance bound β_t is given by

$$\beta_t \triangleq \frac{1}{\alpha_t}\left[1 - \left(1 - \frac{\alpha_t}{N}\right)^N\right] \leq \frac{H(S^G)}{H(S^*)}. \tag{13}$$

From (13) and (11), it is easy to see that: (1) when $\alpha_t \to 1$, $\beta_t \to \beta_f$ (i.e., no improvement); (2) when $\alpha_t \to 0$, $\beta_t \to 1$ (i.e., a significant improvement); and (3) β_t is monotonically decreasing in α_t. Using these three facts and (12), it is easy to see that the improvement in the performance bound is proportional to the magnitude of: $\gamma_t \triangleq \min_{y\in X}\left[\frac{\Delta H(y|X\backslash\{y\})}{\Delta H(y|\emptyset)}\right]$. Note that, the submodularity of H implies $\frac{\Delta H(y|X\backslash\{y\})}{\Delta H(y|\emptyset)} \leq 1, \forall y \in X$. Thus, γ_t is large only when $\frac{\Delta H(y|X\backslash\{y\})}{\Delta H(y|\emptyset)} \simeq 1, \forall y \in X$.

In other words, a significantly improved performance bound from the total curvature measure can only be obtained when H is just "weakly" submodular (i.e., when H is closer to being modular rather than submodular). This is also clear from simplifying the condition $\frac{\Delta H(y|X\backslash\{y\})}{\Delta H(y|\emptyset)} \simeq 1, \forall y \in X$, which leads to the condition:

$$H(X) \simeq H(y) + H(X\backslash\{y\}), \quad \text{for all } y \in X, \tag{14}$$

which holds whenever H is modular.

As H is the set coverage function (6), (14) holds when an agent deployed at any $y \in X$ and all other agents deployed at $X\backslash\{y\}$ contribute to the global coverage objective independently in a modular fashion. This happens when the ground set X is very sparse and/or when the agents have significantly weak non-overlapping sensing capabilities (i.e., small range δ and high decay λ in (1)).

However, (14) is easily violated if $H(X) \ll H(y) + H(X\backslash\{y\})$ for some $y \in X$. To interpret this case using (6), let us consider the analogous detection function (4) requirement: $P(x,X) \ll P(x,\{y\}) + P(x,X\backslash\{y\})$ for some $y \in X$, for a majority of $x \in \Phi$. Now, using (9) and (10) this requirement can be simplified to: $0 \ll \theta(p(x,y)(1 - \prod_{s_i \in X\backslash\{y\}}(1 - p(x,s_i))) + (1-\theta)(\min\{\max_{s_i\in X\backslash\{y\}} p(x,s_i), p(x,y)\})$. Since $\theta \in [0,1]$, we need to consider both terms in the above requirement separately. However, they both lead to a common requirement: $0 \ll p(x,y)$ and $0 \ll p(x,s_i)$, for some $s_i \in X\backslash\{y\}$. In all, the total curvature measure leads to poor performance bounds when there exists some $y \in X$ and $s_i \in X\backslash\{y\}$ so that $0 \ll p(x,y) \simeq p(x,s_i) \simeq 1$, for many feasible space locations $x \in \Phi$. Notably, this condition holds when the ground set X is dense and the agents have significantly strong sensing capabilities (i.e., large range δ and small decay λ in (1)).

One final remark on the total curvature α_t (12) is that it requires an evaluation of $H(X)$ and $M(\triangleq |X|)$ evaluations of $H(X\backslash\{y\})$ terms. In certain coverage applications, this might be ill-defined [9] or computationally expensive as often $H(S)$ is of the complexity $O(|S|\bar{M})$ (where $\bar{M}$ is size of the discretization used to evaluate the coverage integral in (6)).

B. Greedy Curvature [3]

The *greedy curvature* of (6) is given by

$$\alpha_g \triangleq \max_{0\leq i\leq N-1}\left[\max_{y\in X^i}\left(1 - \frac{\Delta H(y|S^i)}{\Delta H(y|\emptyset)}\right)\right], \tag{15}$$

where $X^i \triangleq \{y : y \in X \backslash S^i, (S^i \cup \{y\}) \in \mathscr{I}^N\}$ (i.e., the set of feasible options at the $(i+1)^{\text{th}}$ greedy iteration). The corresponding performance bound β_g is given by

$$\beta_g \triangleq 1 - \alpha_g \left(1 - \frac{1}{N}\right) \leq \frac{H(S^G)}{H(S^*)}. \qquad (16)$$

Note that β_g monotonically decreases with α_g, and $\alpha_g \in [0,1]$ (as H is submodular). Therefore, as $\alpha_g \to 0$, $\beta_g \to 1$, and as $\alpha_g \to 1$, $\beta_g \to \frac{1}{N} < \beta_f$. Using these facts and (15), it is easy to see that the improvement in the performance bound is proportional to the magnitude of $\gamma_g \triangleq \min_{0\leq i \leq N-1}\left[\min_{y\in X^i}\left(\frac{\Delta H(y|S^i)}{\Delta H(y|\emptyset)}\right)\right]$. Similar to before, the submodularity of H implies that γ_g is large only when $\frac{\Delta H(y|S^i)}{\Delta H(y|\emptyset)} \simeq 1, \forall y \in X^i, i \in \mathbb{N}_{N-1}^0$. In other words, similar to the total curvature, the greedy curvature provides a significantly improved performance bound when H is weakly submodular.

In fact, as observed in [9], when H is significantly weakly submodular, it can provide better performance bounds even compared to those provided by the total curvature, i.e., $\beta_f \ll \beta_t \leq \beta_g \simeq 1$. This observation can be theoretically justified using γ_t and γ_g as follows. Due to submodularity, $\Delta H(y|X\backslash\{y\}) \leq \Delta H(y|S^i)$ for any y and S^i, and thus, $\gamma_t \leq \gamma_g$. This, with weak submodularity of H leads to $\alpha_t \geq \alpha_g \simeq 0$. Now, noticing that the growth of β_g is faster as $\alpha_g \to 0$ compared to that of β_t as $\alpha_t \to 0$, we get $\beta_f \ll \beta_t \leq \beta_g \simeq 1$.

We can follow the same steps and arguments as before to show that such improved performance bounds can only be achieved when the ground set is sparse and/or when the agents have weak sensing capabilities. On the other hand, when the ground set is dense and when the agents have strong sensing capabilities, greedy curvature provides poor performance bounds (often, it may even be worse than β_f).

Nevertheless, compared to the total curvature, greedy curvature has wo key redeeming qualities: it is always fully defined, and it can be computed efficiently using only the evaluations of H executed in the greedy algorithm.

C. Elemental Curvature [11]

The *elemental curvature* of (6) is given by

$$\alpha_e \triangleq \max_{\substack{(S,y_i,y_j):S\subset X,\\ y_i,y_j\in X\backslash S,\ y_i\neq y_j.}} \left[\frac{\Delta H(y_i|S\cup\{y_j\})}{\Delta H(y_i|S)}\right]. \qquad (17)$$

The corresponding performance bound β_e is given by

$$\beta_e \triangleq 1 - \left(\frac{\alpha_e + \alpha_e^2 + \cdots + \alpha_e^{N-1}}{1 + \alpha_e + \alpha_e^2 + \cdots + \alpha_e^{N-1}}\right)^N \leq \frac{H(S^G)}{H(S^*)}. \qquad (18)$$

It can be shown that β_e monotonically decreases with α_e, and due to the submodularity of H, $0 \leq \alpha_e \leq 1$. Therefore, when $\alpha_e \to 0$, $\beta_e \to 1$ and when $\alpha_e \to 1$, $\beta_e \to \beta_f$.

According to [7, Prop. 2.1], submodularity of H also implies that $\frac{\Delta H(y_i|S\cup\{y_j\})}{\Delta H(y_i|S)} \leq 1$, for all feasible (S, y_i, y_j) considered in (17). Therefore, when there exists some feasible (S, y_i, y_j) such that $\frac{\Delta H(y_i|S\cup\{y_j\})}{\Delta H(y_i|S)} \simeq 1$, i.e. when H is weakly submodular (closer to being modular) in that region, based on (17), $\alpha_e \simeq 1$ implying $\beta_e \simeq \beta_f$ (i.e., no improvement).

****** Compressed up to this point...**

As explained earlier, H is weakly submodular (which implied $\beta_e \simeq \beta_f$) when the ground set X is very sparse and/or when agents have significantly weak non-overlapping sensing capabilities. Therefore, elemental curvature contrasts from total and greedy curvature - where weakly submodular scenarios led to significantly improved performance bounds $\beta_f \ll \beta_t \leq \beta_g \simeq 1$.

On the other hand, the elemental curvature provides an improved performance bound when $\frac{\Delta H(y_i|S\cup\{y_j\})}{\Delta H(y_i|S)} \ll 1$ over all feasible (S, y_i, y_j) considered in (17). To further interpret this condition, we need to consider the corresponding marginal detection function (8) requirement:

$$\Delta P(x, y_i|S\cup\{y_j\}) \ll \Delta P(x, y_i|S), \quad \forall (S, y_i, y_j) \qquad (19)$$

for a majority of $x \in \Phi$. Since each $\Delta P = \theta \Delta P_J + (1-\theta)\Delta P_M$ where $\theta \in [0,1]$, let us first consider the requirement (19) with respect to the ΔP_J (i.e., when $\theta = 1$ in (**??**)) using (9):

$$\begin{aligned}
&\Delta P_J(x, y_i|S\cup\{y_j\}) \ll \Delta P_J(x, y_i|S)\\
&\iff p(x,y_i)\prod_{s_i\in S\cup\{y_j\}}(1-p(x,s_i)) \ll p(x,y_i)\prod_{s_i\in S}(1-p(x,s_i))\\
&\iff 0 \ll p(x,y_i)p(x,y_j)\prod_{s_i\in S}(1-p(x,s_i)).
\end{aligned}$$

Clearly, this condition holds if for all feasible (S, y_i, y_j),

$$0 \ll p(x,y_i) \simeq p(x,y_j) \simeq 1 \text{ with } 0 \simeq p(x,s_i) \ll 1 \qquad (20)$$

for some $s_i \in S$ over many feasible space locations $x \in \Phi$.

Now, let us consider the requirement (19) with respect to the ΔP_M (i.e., when $\theta = 0$ in (**??**)) using (3):

$$\begin{aligned}
&\Delta P_M(x, y_i|S\cup\{y_j\}) \ll \Delta P_M(x, y_i|S)\\
&\iff \max_{s_i\in S\cup\{y_j,y_i\}} p(x,s_i) - \max_{s_i\in S\cup\{y_j\}} p(x,s_i)\\
&\qquad \ll \max_{s_i\in S\cup\{y_i\}} p(x,s_i) - \max_{s_i\in S} p(x,s_i)\\
&\iff \max_{s_i\in S\cup\{y_j,y_i\}} p(x,s_i) + \max_{s_i\in S} p(x,s_i)\\
&\qquad \ll \max_{s_i\in S\cup\{y_i\}} p(x,s_i) + \max_{s_i\in S\cup\{y_j\}} p(x,s_i). \qquad (21)
\end{aligned}$$

For notational convenience, let $P_S \triangleq \max_{s_i\in S} p(x,s_i)$, $P_{y_i} \triangleq p(x,y_i)$ and $P_{y_j} \triangleq p(x,y_j)$. Then, (21) can be restated as

$$\begin{aligned}
&\max\{P_S, P_{y_i}, P_{y_j}\} + P_S \ll \max\{P_S, P_{y_i}\} + \max\{P_S, P_{y_j}\}\\
&\iff \max\{2P_S, P_S + P_{y_i}, P_S + P_{y_j}\}\\
&\qquad \ll \max\{P_S + \max\{P_S, P_{y_j}\}, P_{y_i} + \max\{P_S, P_{y_j}\}\}\\
&\iff \max\{2P_S, P_S + P_{y_i}, P_S + P_{y_j}\}\\
&\qquad \ll \max\{\max\{2P_S, P_S + P_{y_j}\}, \max\{P_S + P_{y_i}, P_{y_i} + P_{y_j}\}\}\\
&\iff \max\{2P_S, P_S + P_{y_i}, P_S + P_{y_j}\}\\
&\qquad \ll \max\{\max\{2P_S, P_S + P_{y_j}, P_S + P_{y_i}\}, P_{y_i} + P_{y_j}\}\\
&\iff 0 \ll \max\{0, P_{y_i} + P_{y_j} - \max\{2P_S, P_S + P_{y_j}, P_S + P_{y_i}\}\}\\
&\iff \max\{2P_S, P_S + P_{y_j}, P_S + P_{y_i}\} \ll P_{y_i} + P_{y_j}\\
&\iff P_S + \max\{P_S, P_{y_j}, P_{y_i}\} \ll P_{y_i} + P_{y_j}
\end{aligned}$$

Since P_{y_i} and P_{y_j} are interchangeable in the above expression, let us denote $P_y \triangleq P_{y_i} \simeq P_{y_j}$. This makes the above condition:

$$\begin{aligned} & P_S + \max\{P_S, P_y\} \ll 2P_y \\ \iff & \max\{2P_S - 2P_y, P_S - P_y\} \ll 0 \iff P_S \ll P_Y \\ \iff & \max_{s_i \in S} p(x,s_i) \ll p(x,y_i) \simeq p(x,y_j), \end{aligned}$$

which leads to the same condition obtained in (20).

In all, the elemental curvature measure leads to significantly improved performance bounds when for all (S, y_i, y_j) such that $S \subset X, y_i, y_j \in X \backslash S$ and $y_i \neq y_j$,

$$0 \simeq p(x,s_i) \ll p(x,y_i) \simeq p(x,y_j) \simeq 1$$

for some $s_i \in S$ over many feasible space locations $x \in \Phi$. Clearly, this requirement holds when the ground set X is dense and when the agents have significantly strong overlapping sensing capabilities (i.e., large range δ and small decay λ in (1)).

Finally, note that the evaluation of the elemental curvature α_e (17) is computationally expensive (even compared to the total curvature) as it involves solving a set function maximization problem (notice the set variable S in (17)). However, as shown in [10], there may be special structural properties that can be exploited to obtain at least an upper bound on α_e, leading to a lower bound on β_e - which would still be a valid performance bound for the optimal coverage problem (6). The following proposition serves this purpose.

Proposition 1: An upper-bound for the elemental curvature α_e in (17) is given by

$$\alpha_e \leq \bar{\alpha}_e \triangleq 1 - \left(\min_{\substack{(y_i,y_j,x): y_i \in X, y_j \in X\backslash\{y_i\}, \\ x \in \Phi, p(x,y_i) \neq 0}} p(x,y_j) \right) \mathbf{1}_{\{\theta=1\}}. \quad (22)$$

Proof: Due to space constraints, the proof is omitted here, but can be found in [13]. ■

Remark 3: Evaluating the elemental curvature upper-bound $\bar{\alpha}_e$ proposed in (22) is significantly more computationally efficient compared to evaluating the original elemental curvature metric α_e as defined in (17). A valid performance bound for the greedy solution then can be obtained by using the computed $\bar{\alpha}_e$ value to substitute for α_e in (18).

Remark 4: The proposed elemental curvature upper-bound $\bar{\alpha}_e$ proposed in (22) becomes trivial (i.e., $\bar{\alpha}_e = 1$) under two scenarios. The first scenario is when we can place two agents in the mission space ground set (i.e., find $y_i, y_j \in X$) such that there is no overlapping in their sensing regions (i.e., when there exists $x \in \Omega$ such that $p(x,y_i) \neq 0$ but $p(x,y_j) = 0$). The second scenario is when the max detection function is used in the coverage objective (i.e., when $\theta \neq 1$ in (**??**)). Note, however, that the lack of a computationally efficient non-trivial $\bar{\alpha}_e \neq 1$ does not guarantee $\alpha_e = 1$ - as it is just a result of our particular approach used to establish an upper-bound for the elemental curvature α_e. Future research is directed towards addressing these challenges.

D. Partial Curvature [5]

The *partial curvature* of (6) is given by

$$\alpha_p = \max_{(S,y): y \in S \in \mathscr{I}^N} \left[1 - \frac{\Delta H(y|S\backslash\{y\})}{\Delta H(y|\emptyset)} \right]. \quad (23)$$

The corresponding performance bound β_p is given by

$$\beta_p \triangleq \frac{1}{\alpha_p} \left[1 - \left(1 - \frac{\alpha_p}{N} \right)^N \right] \leq \frac{H(S^G)}{H(S^*)}. \quad (24)$$

This partial curvature measure α_p (23) provides an alternative to the total curvature measure α_t (12). In particular, it addresses the potentially ill-defined nature of the $H(X)$ term involved in α_t (12). Consequently, α_p can be evaluated when the domain of H constrained, i.e., when $H : \mathscr{I} \to \mathbb{R}_{\geq 0}$ with some $\mathscr{I} \subset 2^X$.

The above β_p (24) is only valid under a few additional conditions on f, X and $\mathscr{I}^N$ (which are omitted here, but can be found in [5]). Note that we can directly compare α_t and α_p to conclude regarding the nature of the corresponding performance bounds β_t and β_p, as β_t (13) and β_p (24) has identical forms. The work in [5] has established that $\alpha_p \leq \alpha_t$, which implies that $\beta_p \geq \beta_t$, i.e., β_p is always tighter than β_t.

Note also that, similar to β_t, β_p will provide significantly improved performance bounds (i.e., $\beta_p \simeq 1$) when H is weakly submodular. As observed before, such a scenario occurs when the ground set is sparse and/or agent sensing capabilities are weak. On the other hand, again, similar to β_t, β_p will provide poor performance bounds (i.e., $\beta_p \simeq \beta_f$) when H is strongly submodular. This happens when the ground set is dense, and agent sensing capabilities are strong.

Unfortunately, similar to the elemental curvature α_e (17), evaluating the partial curvature α_p (23) involves solving a set function maximization problem (notice the set variable Y in (23)). Therefore, evaluating α_p is much more computationally expensive compared to evaluating α_t or α_g. However, like in the case of α_e, we can exploit some special structural properties of the optimal coverage problem to overcome this challenge.

Proposition 2: An upper-bound for the partial curvature α_p in (23) is given by

$$\alpha_p \leq \bar{\alpha}_p = \frac{1}{\beta_f} \max_{y \in X} \left(1 - \frac{\Delta H(y|A_y^G)}{H(\{y\})} \right) \quad (25)$$

where A_y^G is the greedy solution for the polymatroid maximization (under a uniform matroid constraint) problem

$$A_y^* = \underset{\substack{A \subseteq X\backslash\{y\}, \\ |A| = N-1}}{\arg\max} \left(-\Delta H(y|A) + H(\{y\}) \right). \quad (26)$$

Proof: Due to space constraints, the proof is omitted here, but can be found in [13]. ■

Finally, we point out that the upper bound for α_p established in the above proposition can be computed efficiently, and when used in (24), provides a lower bound to actual partial curvature-based performance bound β_p.

Remark 5: Evaluating the partial curvature upper-bound $\bar{\alpha}_p$ proposed in (25) is significantly more computationally efficient compared to evaluating the original partial curvature metric α_p as defined in (23). A valid performance bound for the greedy solution then can be obtained by using the computed $\bar{\alpha}_p$ value to substitute for α_p in (24).

E. Extended Greedy Curvature [14]

The *extended greedy curvature*, as the name suggests, requires executing some extra greedy iterations in the greedy algorithm (i.e., Alg. 1). This is not an issue as Alg. 1 can be executed beyond N iterations until $M \triangleq |X|$ iterations - analogous to a scenario where more than N agents are to be deployed to the mission space in a greedy fashion.

To define the extended greedy curvature, we first need some additional notations. Recall that we used (S^i, s^i) to denote the greedy (set, element) observed at the i^{th} greedy iteration, where $i \in \mathbb{N}_M^0 \triangleq \mathbb{N}_M \cup \{0\}$. Let $m \triangleq \lfloor \frac{M}{N} \rfloor$, and for any $n \in \mathbb{N}_{m-1}^0$,

$$S_n^G \triangleq S^{(n+1)N} \backslash S^{nN} = \{s^{nN+1}, s^{nN+2}, \ldots, s^{nN+N}\}, \tag{27}$$

$$X_n \triangleq X \backslash S^{nN} \quad \text{and} \quad \mathscr{I}_n^N \triangleq \{S : S \subseteq X_n, |S| \leq N\}. \tag{28}$$

Simply, S_n^G is the $(n+1)^{\text{th}}$ block of size N greedy agent placements, and X_n is the the set of agent locations remaining after nN greedy iterations. Note that, $S_0^G = S^G, X_0 = X$ and $\mathscr{I}_0^N = \mathscr{I}^N$. Note also that, for any $n \in \mathbb{N}_{m-1}^0$, the set system $(X_n, \mathscr{I}_n^N)$ is a uniform matroid of rank N, and S_n^G is the greedy solution for $\arg\max_{S \in \mathscr{I}_n^N} H(S)$.

The extended greedy curvature of (6) is given by

$$\alpha_u \triangleq \min_{i \in Q} \ \alpha_u^i, \tag{29}$$

where $Q \subseteq \bar{Q} \triangleq \{i \in \mathbb{N}_M : i = nN+1, \ n \in \mathbb{N}_{m-1}^0 \text{ or } i = nN, \ n \in \mathbb{N}_m \text{ or } i = M\}$ and

$$\alpha_u^i \triangleq \begin{cases} H(S^{i-1}) + \max\limits_{S \in \mathscr{I}_{(i-1)/N}^N} \left[\sum_{y \in S} \Delta H(y|S^{i-1})\right] \\ \qquad \text{if } i = nN+1, \ n \in \mathbb{N}_{m-1}^0, \\ H(S^{i-N}) + \frac{1}{\beta_f}\left[H(S^i) - H(S^{i-N})\right] \\ \qquad \text{if } i = nN, \ n \in \mathbb{N}_m, \\ H(S^i) \qquad \text{if } i = M. \end{cases} \tag{30}$$

The performance bound β_u corresponding to the extended greedy curvature measure α_u is given by

$$\beta_u \triangleq \frac{H(S^G)}{\alpha_u} \leq \frac{H(S^G)}{H(S^*)}. \tag{31}$$

Note that $\bar{Q}$ is a fixed set of greedy iteration indexes. For each $i \in \bar{Q}$, a corresponding α_u^i value can be computed using known byproducts generated during the execution of greedy iterations. Unlike $\bar{Q}$, Q is an arbitrary subset selected from $\bar{Q}$ based on the user preference. For example, one may choose $Q = \{1, N, N+1, 2N, 2N+1\}$ so that α_u value can be obtained upon executing only $N+1$ extra greedy iterations. Another motivation for selecting a smaller set for Q compared to $\bar{Q}$ may also be the computational cost associated with running extra greedy iterations.

However, according to (31), β_u is a monotonically decreasing function in α_u, and according to (29), α_u is a monotonically decreasing set function in Q. Consequently, the performance bound β_u is a *monotone set function* in Q, implying that any superset of Q will always provide a better (or at least the same) β_u value compared to that obtained from the set Q.

In the context of optimal coverage problem (6), to identify unique qualities of this extended greedy curvature-based performance bound, let us first consider α_u^1 (from (30)):

$$\alpha_u^1 = H(S^0) + \max_{S \in \mathscr{I}_0^N} \left[\sum_{y \in S} \Delta H(y|S^0)\right] = \max_{S \in \mathscr{I}^N} \left[\sum_{y \in S} H(y)\right]$$

Notice that when the set coverage function H is closer to being modular (i.e., weakly submodular), the above $\alpha_u^1 \simeq H(S^*)$. Through (29) and (31), this implies that $\frac{H(S^G)}{\beta_u} = \alpha_u \leq \alpha_u^1 \simeq H(S^*)$, leading to the conclusion $\beta_u \simeq 1$. Therefore, when H is weakly submodular, i.e., when the ground set is sparse and/or agent sensing capabilities are weak, β_u provides significantly improved performance bounds. This bahaviour is similar to that of the performance bounds β_t, β_g and β_p discussed before.

Let us now consider α_u^{2N} (from (30), also using $S^N = S^G$)

$$\alpha_u^{2N} = H(S^G) + \frac{1}{\beta_f}\left[H(S^{2N}) - H(S^N)\right]. \tag{32}$$

Notice that when the set coverage function H is strongly submodular (i.e., when its "diminishing returns" property is severe, see Def. 1(3)), the greedy coverage level $H(S^i)$ should saturate quickly with the greedy iterations i. Consequently, above $\alpha_u^{2N} \simeq H(S^G)$ as $\frac{1}{\beta_f}(H(S^{2N}) - H(S^N)) \simeq 0$. Through (29) and (31), this implies that $\frac{H(S^G)}{\beta_u} = \alpha_u \leq \alpha_u^1 \simeq H(S^G)$ leading to the conclusion $\beta_u \simeq 1$. Therefore, when H is strongly submodular, i.e., when the ground set is dense, and agent sensing capabilities are strong, β_u provides significantly improved performance bounds. This bahavior is similar to that of the performance bound β_e discussed before.

Moreover, in this strong submodular case, as $\beta_f \ll \beta_e \simeq 1$, it is worth noting that the above factor $\frac{1}{\beta_f}$ (originally appearing in (30)) can be replaced with the much smaller factor $\frac{1}{\beta_e}$ (compared to $\frac{1}{\beta_f}$). Therefore, this modification leads to further improvements in the performance bound $\beta_u \simeq 1$.

In all, the extended greedy curvature measure-based performance bound β_u is computationally efficient and provides significantly improved performance bounds under both strong and weak submodular scenarios. This behavior contrasts with that of all other performance bounds discussed before.

V. Discussion

In this section, we summarize our findings on the effectiveness and computational complexity of different curvature-based performance bounds in optimal coverage problems. In particular, our findings have been summarized in Tab. I.

In terms of effectiveness, we have observed that total, greedy, and partial curvature measures provide significantly improved performance bounds when agents have low sensing capabilities (i.e., high decay λ and/or low range δ) and/or

TABLE I: Characteristics of different curvature-based performance metrics in the context of optimal coverage problems

β	$\beta_f \ll \beta \simeq 1$ when:				Complexity	Remarks
	Agent Sensing (1)		Denseness of X			$H(S) \sim O(\lvert S\rvert \bar{M})$
	Low $\delta \downarrow, \lambda \uparrow$	High $\delta \uparrow, \lambda \downarrow$	Low $(M \downarrow)$	High $(M \uparrow)$		Alg. 1 $\sim O(N^2 M \bar{M})$
β_t	✓	✗	✓	✗	$O(M^2\bar{M})$	
β_g	✓	✗	✓	✗	$O(N)$	
β_e	✗	✓	✗	✓	$O(M^3 2^M \bar{M})$	Estimate (22): $O(M^2\bar{M})$
β_p	✓	✗	✓	✗	$O(M^N \bar{M})$	Estimate (25): $O(N^2 M^2 \bar{M})$
β_e	✓	✓	✓	✓	$O(n^2 N^2 M \bar{M})$	(i.e., for nN extra iter.) Worst Case: $O(M^3\bar{M})$

when the ground set is sparse (i.e., low M). In particular, compared to the total curvature, (1) greedy curvature performs slightly better in such "weakly submodular" scenarios, and (2) partial curvature performs slightly better in general. Conversely, the elemental curvature measure provides significantly improved performance bounds when agents have strong sensing capabilities (i.e., low decay λ and/or high range δ) and/or when the ground set is dense (i.e., high M). Most importantly, the extended greedy curvature distinguishes itself by being able to provide significantly improved performance bounds regardless of the nature of agent sensing capabilities or ground set denseness - proving its versatility in a broad range of scenarios.

In terms of computational complexity, the greedy curvature measure is the most efficient as it can be computed directly using the byproducts of the greedy algorithm (it has a complexity $(O(N))$). The total curvature exhibits a complexity of $O(M^2\bar{M})$, manageable but higher than greedy curvature. The conservative upper-bound estimate of the elemental curvature has the same complexity $O(M^2\bar{M})$. In contrast, the original elemental and partial curvatures measures have the highest computational complexities, $O(M^3 2^M \bar{M})$ and $O(M^N \bar{M})$ (i.e., without some constraints, $O(M^3 2^M \bar{M})$), respectively. The conservative upper-bound estimate of the partial curvature has a higher complexity $O(M^2 2^M \bar{M})$ than that for elemental curvature. The complexity of extended greedy curvature is less considerable compared to that of elemental and partial curvature. However, it is of comparable complexity with respect to that of total curvature and conservative upper bound estimates of elemental and partial curvature measures.

To summarize, this review has highlighted three main challenges in using curvature-based performance bounds for optimal coverage problems: (1) the inherent dependence of the effectiveness on the strong or weak nature of the submodularity property of the considered optimal coverage problem, (2) the computational complexity associated with computing the curvature measures, and (3) the technical conditions required for the successful application of curvature-based performance bounds (e.g., see Remark 4). Towards addressing these challenges, the recently proposed extended greedy curvature concept [14] has shown promising advances. This curvature measure takes a data-driven approach and utilizes only the information observed during a selected number of extra greedy iterations - offering a computationally efficient performance bound without inherent or technical limitations.

In light of these findings, we believe future research should be directed toward finding more *data-driven curvature measures* (e.g., α_u) to directly address computational challenges faced by standard *theoretical curvature measures* (e.g., α_e, α_p). However, in such a pursuit, like in any other data-driven technique development, a crucial challenge would be to establish theoretical guarantees/characterizations on its effectiveness/performance. This challenge motivates exploring *hybrid curvature measures* that have elements rooted in both data-driven curvature measures and theoretical curvature measures.

In a limited sense, the extended greedy curvature measure α_u can be seen as a hybrid curvature measure as it involves a term β_f in (30) that can be replaced by β_t, β_e or β_p (which are functions of *theoretical curvature measures* α_t, α_e or α_p, respectively). On the other hand, the developed computationally efficient upper bounds on theoretical curvature measures using data-driven techniques (e.g., see $\bar{\alpha}_p$ proposed in Prop. 2) can also be seen as a hybrid curvature measure. Nevertheless, the complete theoretical implications of such hybrid curvature measures are yet to be studied, not only in the context of optimal coverage problems but also in the context of broader submodular maximization problems.

VI. Case Studies

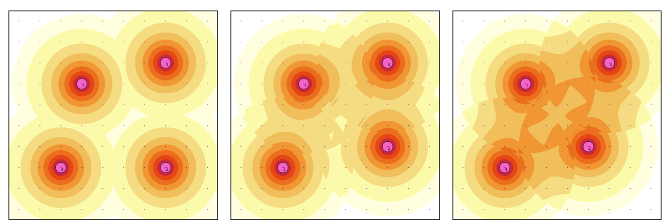

(a) $\theta = 0, \beta_u = 0.84$ (b) $\theta = 0.5, \beta_u = 0.87$ (c) $\theta = 1, \beta_u = 0.92$

Fig. 1: Greedy solutions, coverage level patterns, and the tightest performance bounds observed under different weight parameters $\theta \in [0, 1]$ in the Blank mission space with $N = 4$ agents with sensing range $\delta = 200$ and decay $\lambda = 0.012$.

In our numerical experiments, we considered square-shaped mission spaces (each side is of length 600 units) with three different obstacle arrangements named "Blank," "Maze" and "General" as can be seen in Figs. 1-2, 3 and **??**, respectively. Note that, in such figures, obstacles are shown as dark green-colored blocks, candidate agent locations (ground set X) are shown as small black dots, and agent locations are shown as numbered pink-colored circles. Note also that light-colored areas indicate low coverage (i.e., low event detection probability) levels, while dark-colored areas indicate the opposite. The event density function was assumed to be uniform, i.e., $R(x) = 1, \forall x \in \Phi$.

The main attributes and functionalities of the considered class of multi-agent optimal coverage problems (e.g., agent sensing capabilities (1) and functions like detection (4) and coverage (5)) as well as the greedy algorithm (Alg. 1) and the reviewed performance bounds β_f (11), β_t (13), β_g (16), β_e (18), β_p (24) and β_u (31) were all

TABLE II: Performance bounds observed under different sensing decay λ values in the Blank mission space with $N = 10$ agents with sensing range $\delta = 800$.

Perf. bounds with respect to θ at $\lambda = 0.05$						
θ	β_f	β_t	β_g	β_e	β_p	β_u
0	0.651	0.745	0.595	0.651	0.676	**0.943**
0.5	0.651	0.790	0.753	0.651	0.753	**0.965**
1	0.651	**0.840**	**0.872**	0.651	**0.829**	**0.992**
Perf. bounds with respect to λ at $\theta = 0.5$						
λ	β_f	β_t	β_g	β_e	β_p	β_u
0.05	0.651	**0.790**	**0.753**	0.651	**0.753**	**0.965**
0.045	0.651	0.765	0.714	0.651	0.720	**0.951**
0.04	0.651	0.739	0.669	0.651	0.686	**0.930**
0.035	0.651	0.713	0.617	0.651	0.651	**0.901**
0.3	0.651	0.689	0.559	0.651	0.651	**0.857**
0.025	0.651	0.670	0.493	0.651	0.651	**0.795**
0.02	0.651	0.659	0.416	0.651	0.651	**0.705**
0.015	0.651	0.655	0.324	0.651	0.651	**0.656**
0.01	0.651	0.653	0.214	0.651	0.651	**0.742**
0.005	0.651	0.652	0.118	0.651	0.651	**0.912**
0.003	0.651	0.651	0.103	0.651	0.651	**0.954**
0.001	0.651	0.651	0.100	0.651	0.651	**0.986**
Perf. bounds with respect to θ at $\lambda = 0.001$						
θ	β_f	β_t	β_g	β_e	β_p	β_u
0	0.651	**0.651**	**0.101**	0.651	0.651	**0.967**
0.5	0.651	0.651	0.100	0.651	0.651	**0.986**
1	0.651	0.651	0.100	**0.998**	0.651	**1.000**

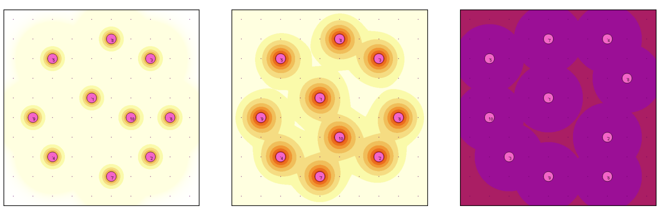

(d) $\lambda = 0.05$ (e) $\lambda = 0.025$ (f) $\lambda = 0.001$

Fig. 2: Greedy solutions and coverage level patterns observed under different sensing decay λ values considered in Tab. II.

TABLE III: Performance bounds observed under different sensing range δ values in the Maze mission space with $N = 10$ agents with sensing range $\lambda = 0.012$.

Perf. bounds with respect to θ at $\delta = 50$						
θ	β_f	β_t	β_g	β_e	β_p	β_u
0	0.651	0.694	0.682	0.651	0.651	**0.992**
0.5	0.651	0.718	0.729	0.651	0.651	**0.992**
1	0.651	**0.742**	**0.775**	0.651	**0.672**	**0.992**
Perf. bounds with respect to δ at $\theta = 0.5$						
δ	β_f	β_t	β_g	β_e	β_p	β_u
50	0.651	**0.718**	**0.729**	0.651	**0.651**	**0.992**
100	0.651	0.660	0.401	0.651	0.651	**0.976**
150	0.651	0.657	0.347	0.651	0.651	**0.919**
200	0.651	0.657	0.342	0.651	0.651	**0.892**
250	0.651	0.656	0.340	0.651	0.651	**0.868**
300	0.651	0.656	0.329	0.651	0.651	**0.847**
350	0.651	0.656	0.329	0.651	0.651	**0.841**
400	0.651	0.656	0.329	0.651	0.651	**0.837**
500	0.651	0.656	0.329	0.651	0.651	**0.835**
600	0.651	0.656	0.328	0.651	0.651	**0.828**
700	0.651	0.656	0.329	0.651	0.651	**0.834**
800	0.651	0.656	0.329	0.651	0.651	**0.834**
Perf. bounds with respect to θ at $\delta = 800$						
θ	β_f	β_t	β_g	β_e	β_p	β_u
0	0.651	**0.660**	0.191	0.651	0.651	**0.789**
0.5	0.651	0.656	0.329	0.651	0.651	**0.834**
1	0.651	0.652	**0.460**	0.651	0.651	**0.898**

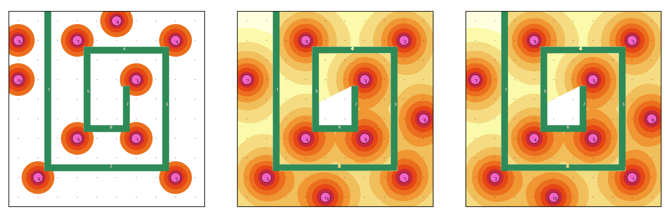

(a) $\delta = 50$ (b) $\delta = 350$ (c) $\delta = 800$

Fig. 3: Greedy solutions and coverage level patterns observed under different sensing range δ values considered in Tab. III.

implemented for the considered class of multi-agent optimal coverage problems in an interactive JavaScript-based simulator which is available at `https://github.com/shiran27/P2-Submod_Coverage`. This simulator may be used by the reader to reproduce the reported results and also to try different new problem configurations.

For evaluating the performance bounds β_e and β_p, we used the proposed techniques in Props. 1 and 2, respectively. Unlike sampling-based techniques used in prior work, these techniques are computationally efficient and provide theoretically valid performance bounds. For evaluating the performance bound β_u, we used $Q = \bar{Q}$ in (29) as in [14].

A. Impact of the Weight Parameter θ

First, we demonstrate the effects of the weight parameter θ (see the detection function in (4)) using the Blank mission space with $N = 4$ agents. Here, each agent is assumed to have a sensing range $\lambda = 200$ and a sensing decay $\delta = 0.012$ (see the sensing function in (1)). The observed greedy solution, coverage level pattern, and performance bounds, when this weight parameter is varied from $\theta = 0$ to $\theta = 1$, are reported in Fig. 1.

As stated in Rm. 1, choosing $\theta = 1$ (i.e., promoting joint detection (2)) motivates cooperation while choosing $\theta = 0$ (i.e., promoting max detection (3)) motivates compartmentalization in sensing. This behavior is confirmed by the observations reported in Fig. 1. In particular, as can be seen in Fig. 1(a), when $\theta \simeq 0$, agents are spread out in the mission space - leaving a blind region in the middle but covering a wider area in the mission space. On the other hand, as can be seen in Fig. 1(e), when $\theta \simeq 1$, agents are located relatively closer to each other than before - not leaving a blind region in the middle but failing to adequately cover some outer regions of the mission space.

Besides such implications, as can be seen from the performance bounds reported in Figs. 1(a)-(e), the weight parameter θ also affect the performance bounds. In particular, the performance bound β_u (which, in this case, offers the highest performance bound) increases with θ. This behavior implies that, with respect to the used greedy solution approach, the optimal coverage problem defined with a max detection function (3) is harder to solve than that with a joint detection function (2). This conclusion is intuitive as max detection functions significantly increase the non-smooth nature of the optimal coverage problems.

Note that, in the numerical examples discussed in the sequel, we predominantly used $\theta = 0.5$. However, in a few extreme cases, as can be seen in the top and bottom sub-tables in Tabs. **??**-**??**, we have further investigated the effect of θ on different performance bounds.

B. Impact of Agent Sensing Capabilities δ, λ

We next demonstrate the impact of the agent sensing capabilities (characterized by their sensing range δ and sensing decay λ) on different curvature-based performance bounds established for greedy solutions. For this purpose, we first use the Blank mission space with $N = 10$ agents. In one experiment, we kept the agent sensing decay fixed at $\lambda = 0.003$ and varied the sensing range from $\delta = 35$ to $\delta = 800$. The observed performance bounds and a few selected greedy solutions are reported in Tab. **??** and the accompanying Fig. **??**, respectively. In the second experiment, we kept the agent sensing range fixed at $\delta = 800$ and varied the sensing decay from $\lambda = 0.05$ to $\delta = 0.001$. The observed performance bounds and a few selected greedy solutions are reported in Tab. **??** and the accompanying Fig. **??**, respectively.

With regard to Tabs. **??** and II, notice that we have further explored the impact of θ at the extreme cases, i.e., when $\delta \in \{35, 800\}$ and $\lambda \in \{0.05, 0.001\}$, respectively. The observations in each case are given in smaller sub-tables located above and below the main table. In each table (and sub-table), the highest performance bound values observed in each row and column have been highlighted for the convenience of the reader. Note also that the tables are arranged in such a way that when going from top to bottom, the sensing capabilities of the agents increase (i.e., δ increase and λ decrease).

Recall that, based on our analysis, the performance bounds β_t, β_g, β_p, and β_u should provide significant improvements beyond β_f when agent sensing capabilities are low (i.e., when δ is low and λ is high). The results in Tabs. **??** and II validate this conclusion (e.g., see the respective results for $\delta = 35$ and $\lambda = 0.05$).

On the other hand, our analysis implied that the performance bounds β_e and β_u should provide significant improvements beyond β_f when agent sensing capabilities are high (i.e., when δ is high and λ is low). With regard to β_e, as mentioned in Rm. 4, we also need the additional condition $\theta = 1$. Again, the results in Tabs. **??** and II validate this conclusion (e.g., see the respective results for $\delta = 800$ and $\lambda = 0.001$, particularly with $\theta = 1$).

Moreover, as expected from our analysis, the observations in Tabs. **??** and II also confirms that the performance bound β_u provide significant improvements beyond β_f regardless of the agent sensing capabilities. Of course, there is a small region of moderate agent sensing capabilities for which this improvement is low (yet, still considerable), e.g., see the respective results for $100 \leq \delta \leq 150$ and $0.01 \leq \lambda \leq 0.02$.

Finally, we consider mission spaces with obstacles, in particular, the Maze and General mission spaces, with $N = 10$ agents. Parallel to the previous two experiments, in one experiment, we kept the agent sensing decay fixed at $\lambda = 0.012$ and varied the sensing range from $\delta = 50$ to $\delta = 800$. The observed performance bounds and a few selected greedy solutions are reported in Tab. III and the accompanying Fig. 3, respectively. In the next experiment, we kept the agent sensing range fixed at $\delta = 200$ and varied the sensing decay from $\lambda = 0.05$ to $\delta = 0.001$. The observed performance bounds and a few selected greedy solutions are reported in Tab. **??** and the accompanying Fig. **??**, respectively.

Using the results reported in Tabs. III and **??**, we can validate all the previous conclusions. The only notable exception here is that the performance bound β_e now provides no improvements. This is due to the presence of obstacles that violate the requirement stated in Rm. 4.

VII. Conclusion

In this paper, we considered a generalized class of multi-agent optimal coverage problems and established its several polymatroid features. These properties enabled efficient solving of the considered optimal coverage problem via greedy algorithms with performance-bound guarantees. To obtain further improved performance bounds, we reviewed five curvature measures found in the literature. In particular, we identified their effectiveness and computational complexity features and proposed novel techniques to estimate efficient candidates for some of such curvature measures. We also implemented the proposed coverage problem in an interactive simulator along with its greedy solutions, and performance bounds. The obtained numerical results validated our findings. Ongoing research activities explore meaningful ways to combine the strengths of data-driven and theoretical curvature measures.

References

[1] E Boros, K Elbassioni, V Gurvich, and L Khachiyan. An Inequality for Polymatroid Functions and its Applications. *Discrete Applied Mathematics*, 131(2):255–281, 2003. doi:10.1016/S0166-218X(02)00455-9.

[2] Reuven Cohen and Liran Katzir. The Generalized Maximum Coverage Problem. *Information Processing Letters*, 108(1):15–22, 2008. doi:10.1016/j.ipl.2008.03.017.

[3] Michele Conforti and Gérard Cornuéjols. Submodular Set Functions, Matroids and The Greedy Algorithm: Tight Worst-Case Bounds and Some Generalizations of The Rado-Edmonds Theorem. *Discrete Applied Mathematics*, 7(3):251–274, 1984.

[4] Gerard Corneuejols, Marshall L. Fisher, and George L. Nemhauser. Location of Bank Accounts to Optimize Float: An Analytic Study of Exact and Approximate Algorithms. *Management Science*, 23(8):789–810, 1977. doi:10.1287/mnsc.23.8.789.

[5] Yajing Liu, Edwin K P Chong, and Ali Pezeshki. Improved Bounds for The Greedy Strategy in Optimization Problems with Curvature. *Journal of Combinatorial Optimization*, 37(4):1126–1149, 2018.

[6] Wenhao Luo and Katia Sycara. Voronoi-Based Coverage Control with Connectivity Maintenance for Robotic Sensor Networks. In *Intl. Symp. on Multi-Robot and Multi-Agent Systems*, pages 148–154, 2019. doi:10.1109/MRS.2019.8901078.

[7] G. L. Nemhauser, L A. Wolsey, and M.L. Fisher. An Analysis of Approximations for Maximizing Submodular Set Functions—I. *Mathematical Programming*, 14(1):265–294, 1978.

[8] Navid Rezazadeh and Solmaz S. Kia. A Sub-Modular Receding Horizon Approach to Persistent Monitoring for A Group of Mobile Agents Over an Urban Area. In *IFAC-PapersOnLine*, volume 52, pages 217–222, 2019.

[9] Chuangchuang Sun, Shirantha Welikala, and Christos G. Cassandras. Optimal Composition of Heterogeneous Multi-Agent Teams for Coverage Problems with Performance Bound Guarantees. *Automatica*, 117:108961, 2020. `doi:10.1016/j.automatica.2020.108961`.

[10] Xinmiao Sun, Christos G Cassandras, and Xiangyu Meng. Exploiting Submodularity to Quantify Near-Optimality in Multi-Agent Coverage Problems. *Automatica*, 100:349–359, feb 2019.

[11] Zengfu Wang, Bill Moran, Xuezhi Wang, and Quan Pan. Approximation for Maximizing Monotone Non-Decreasing Set Functions with A Greedy Method. *Journal of Combinatorial Optimization*, 31(1):29–43, 2016.

[12] Shirantha Welikala and Christos G. Cassandras. Distributed Non-Convex Optimization of Multi-Agent Systems Using Boosting Functions to Escape Local Optima. *IEEE Trans. on Automatic Control*, 2020. `doi:10.1109/TAC.2020.3034869`.

[13] Shirantha Welikala and Christos G Cassandras. Performance-Guaranteed Solutions for Multi-Agent Optimal Coverage Problems using Submodularity, Curvature, and Greedy Algorithms. *arXiv e-prints*, page xxxx.xxxxx, 2023. URL: `http://arxiv.org/abs/xxxx.xxxxx`, `arXiv:xxxx.xxxxx`.

[14] Shirantha Welikala, Christos G. Cassandras, Hai Lin, and Panos J. Antsaklis. A New Performance Bound for Submodular Maximization Problems and Its Application to Multi-Agent Optimal Coverage Problems. *Automatica*, 144:110493, 2022. `doi:10.1016/j.automatica.2022.110493`.

[15] Dengxiu Yu, Hao Xu, C L Philip Chen, Wenjie Bai, and Zhen Wang. Dynamic Coverage Control Based on K-Means. *IEEE Trans. on Industrial Electronics*, 69(5):5333–5341, 2022. `doi:10.1109/TIE.2021.3080205`.

[16] M Zhong and C G Cassandras. Distributed Coverage Control and Data Collection with Mobile Sensor Networks. *IEEE Trans. on Automatic Control*, 56(10):2445–2455, 2011.